Publ. Astron. Obs. Belgrade No. 86 (2009), 117 - 123 *Contributed paper*

BINARY CLUSTERS OBSERVED WITH XMM-NEWTON X-RAY OBSERVATORY

B. BEYGU[1], M. HUDAVERDI[2] and N. ERCAN[1]

[1]*Boğaziçi University, Physics Department, 34342 Istanbul, Turkey*
E–mail: burcu.beygu@boun.edu.tr

[2]*TUBITAK, Space Technologies, Research Institute ODTU, 06531 Ankara, Turkey*

Abstract. Clusters of galaxies are thought to form by accretion of galaxies along the cosmic filaments, and merging of clusters formed earlier. Observations and hydrodynamic simulations show the strong effects of mergers on physical conditions of the Intra Cluster Medium (ICM). In this work, we investigate five relatively nearby Abell clusters; A3705 (z= 0.089), A2440 (z= 0.090), A2933 (z= 0.092), A3888 (z= 0.152) and A115 (z= 0.193). Temperature and metal abundance map are created using wavelet algorithms. Peculiar regions are spectrally studied and large scale of deviations are observed. Based on the results merging histories of our cluster sample are interpreted.

1. INTRODUCTION

Clusters of galaxies are large scale structures in the Universe with radiation powers of the order of 10^{43}–10^{46} erg s^{-1}. They are formed from the gravitational collapse of the field galaxies and the subgroups. X-ray observations have provided us a detailed knowledge on the cluster structure, composition, and formation history. Optical point of view defines clusters of galaxies only as a collection of galaxies. But the X-ray observations show that clusters are continuous structures, known as intracluster medium (ICM). ICM, which is a hot plasma at temperatures of 10^6–10^8 K, fills the whole volume and determines the shape of the cluster. Thus X-ray studies of the ICM are very important for the understanding of dynamical evolution of the clusters of galaxies (Böhringer 2008, The Universe in X-Ray, Springer). Some clusters show sub-structures in X-ray and optical domains. Binary clusters are such clusters for which we can see two poles as a diffuse shape in their X-ray images. The ICM is more dynamic in binary environment, because merger effect shocks and creates turbulent plasma. In this work, we analyzed five binary clusters of galaxies (see Table 1 for the observation log) by means of temperature and metal distributions, in order to understand their dynamical structures. We adopted the Hubble constant H_0=50 km s^{-1} Mpc^{-1}, and a cosmological deceleration parameter of $q_0 = 0.5$. Unless otherwise stated, errors are quoted at 1σ and abundances are given in solar units (Anders and Grevesse 1989).

2. ANALYSIS

We used the X-ray data obtained using the XMM-*Newton* observations. Table 1 shows the observations log. The three European Photon Imaging Camera (EPIC) instruments, the two MOS detector and the PN detector, were used. The event lists were generated from the Observation Data Files (ODF) by Science Analysis System (SAS) version 7.1.0. Wavelet maps are created by using the algorithm package built by Bourdin (Bourdain et al. 2004), which is designed for the mapping of ICM emissivity and temperature. We then selected the events with single and double pixel. In order to clean the contamination by soft proton flares, extracted light curves are clipped by 2.7σ (90%) of the average count rate (Pratt et al. 2003). Since ICM covers large portion of field of view on the EPIC CCDs, background is a challenging issue for clusters. Blank-sky observations, which are superposition of field observations, can be used as background but they include unknown level of instrumental and cosmic contamination. Thus, we extract the local background from each observations for PN CCDs and used XMM-ESAS for MOS CCDs (Snowden et al. 2007). X-ray images and related contours are produced from 0.8-8.8 keV all band images, are not corrected for exposure and background. Optical images are obtained from DSS B-filter archive. For the binary sample, the spectra are studied in the 0.8-8.0 keV energy range with XSPEC v12. The spectral model used in the fitting is APEC thermal plasma model. Instrumental gaussian lines are included if needed.

Table 1: Observation log of the analyzed sources from XMM- *Newton* archive.

Source	z	α	δ	*Exposure*	*obs_id*
Abell 3705	0.089	$20^h42^m00^s.72$	$-35^o13'54''.8$	24.610 ks	0203020201
Abell 2440	0.090	$22^h23^m49^s.34$	$-01^o37'48''.3$	46.711 ks	0401920101
Abell 2933	0.092	$01^h40^m41^s.05$	$-54^o34'33''.6$	31.811 ks	0305060101
Abell 3888	0.152	$22^h34^m34^s.07$	$-37^o43'06''.9$	21.213 ks	0404910801
Abell 0115	0.193	$00^h55^m50^s.48$	$+26^o24'43''.1$	44.809 ks	0203220101

Abell 3705: This is an *irregular* cluster with a bright cD galaxy (Gonzalez et al. 2005). It was observed with a total exposure time of 24.61 ks, in 2004. We display raw merged images (MOS and PN) and the optical image overlaid by X-ray contours in Fig. 1. The cD galaxy associated with X-ray peak of southern pole is evident. Wavelet temperature and abundance maps (see Fig. 2) show that the binary peaks have significantly higher temperature than the region in between. The spectral analysis confirms that A and B ($\sim$ 2.5 keV) are hot compared to region C (1.3 keV). The region A has 0.35 solar abundance value, while for the regions B and C the values are relatively low (0.05 solar).

Abell 2440: This is an *intermediate* cluster of richness class 0 (Mohr et al. 1996). It was observed for exposure time of 46.7 ks, with the medium filter. Fig. 3 (a) shows the raw MOS and PN images with the region of interests and (b) optical DSS image with superposed X-ray contours. Both A2440-NE and A2440-SW X-ray peaks are associated with a bright cD elliptical. The temperature and metal distribution maps (Fig. 4) show small scale variations. The region between the peaks of A2440-NE region (3.9 keV) and A2440-SW (3.2 keV) has a higher temperature value of 4.2 keV. Interestingly, it shows a lower metallicity value of 0.37 solar, compared to NE and SW peaks (0.63 and 0.68 solar, respectively).

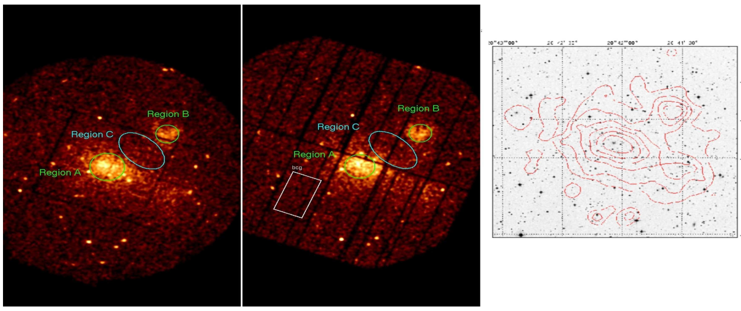

Figure 1: A3705: (a) EPIC images. (b) Optical image with red X-ray contours.

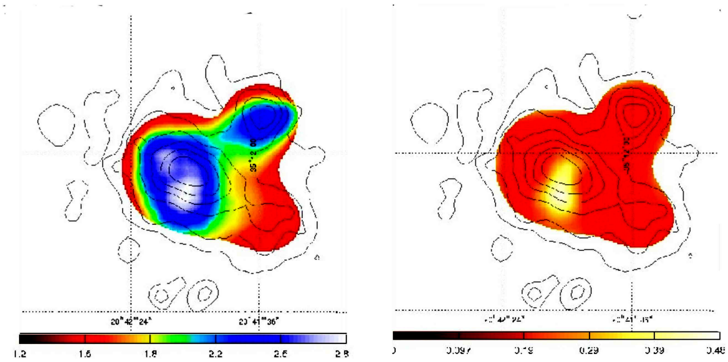

Figure 2: A3705: (a) temperature, (b) metal distribution maps.

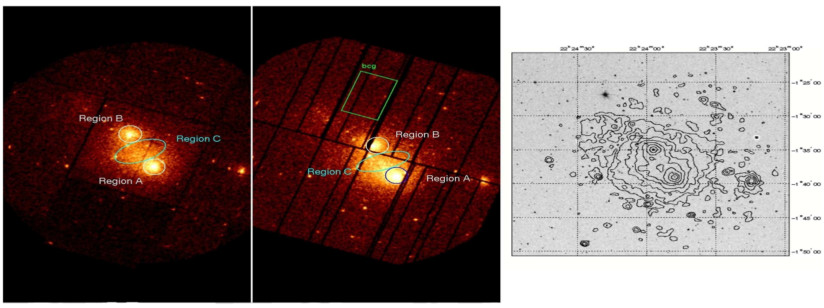

Figure 3: A2440: (a) EPIC images. (b) X-ray contours over optical image.

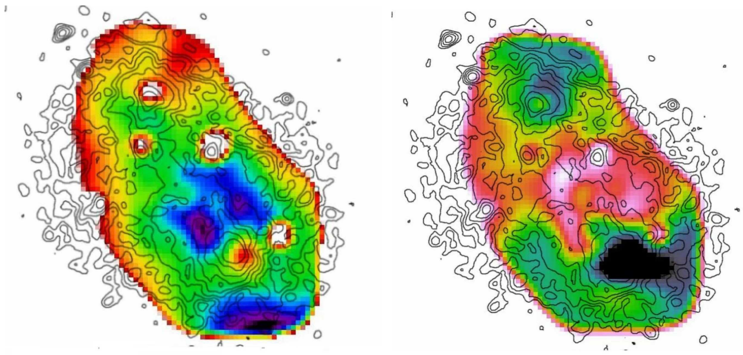

Figure 4: A2440: (a) Temperature map (b) metal abundance map.

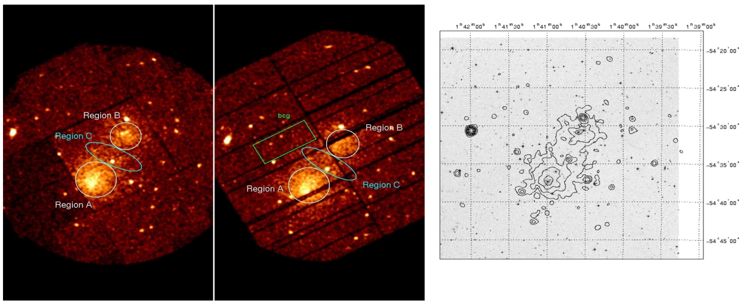

Figure 5: A2933: (a) EPIC images (b) X-ray contours over optical image.

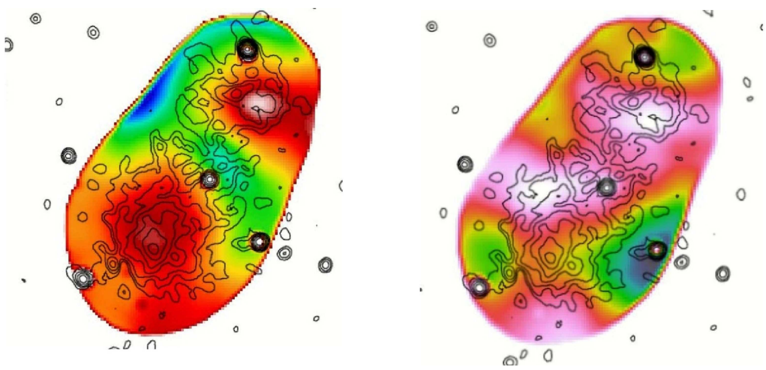

Figure 6: A2933: (a) Temperature map (b) metal abundance map.

Abell 2933: This is a *regular-intermediate* (RI) type cluster and its Bautz-Morgan type is *III* (Kolokotronis et al. 2001). It was observed with a total exposure time of 31.811 ks, 2005. The EPIC raw images and DSS B-filter image of the region are shown in Fig. 5. The wavelet map of temperature and metal abundances are displayed in Fig. 6. A2933-A and A2933-B have X-ray plasma in between with a higher temperature. The metal abundance value is very low in ICM.

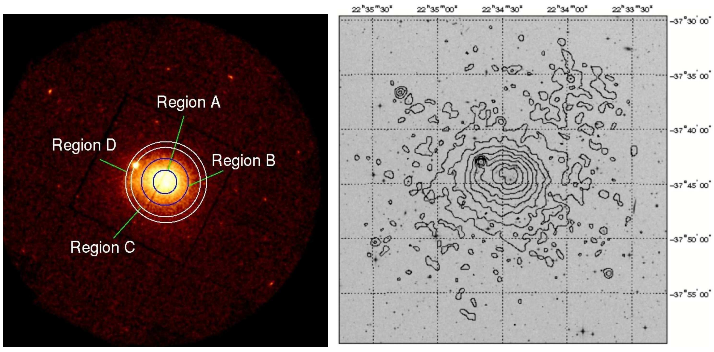

Figure 7: A3888: (a) EPIC images, (b) DSS optical image.

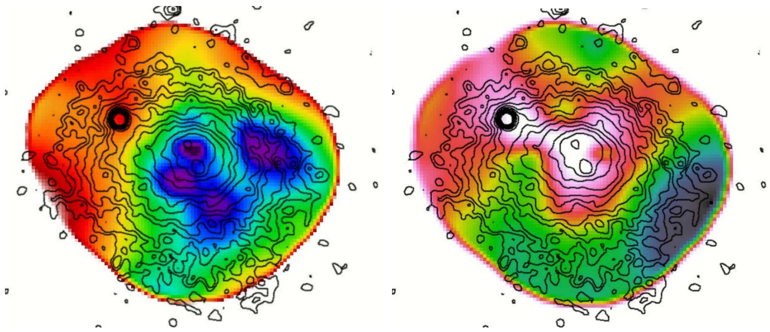

Figure 8: A3888: (a) Temperature map and (b) metal abundance map.

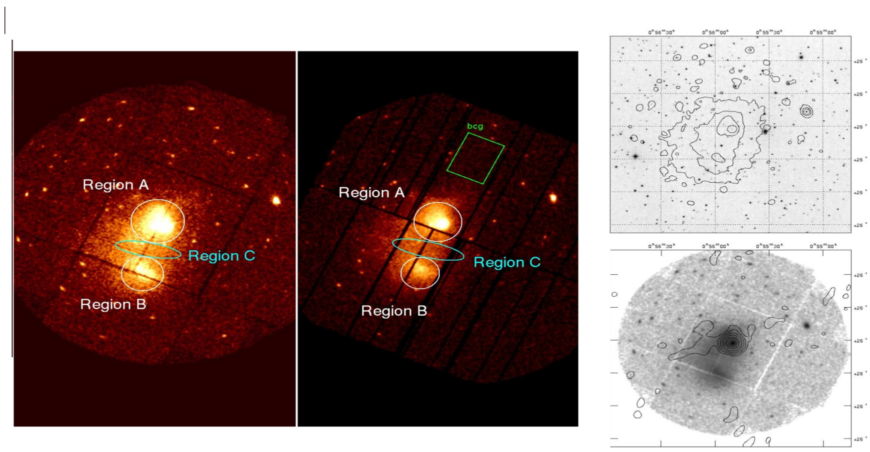

Figure 9: Abell 115: Raw EPIC X-ray image, optical image and radio contours superimposed on the X-ray image.

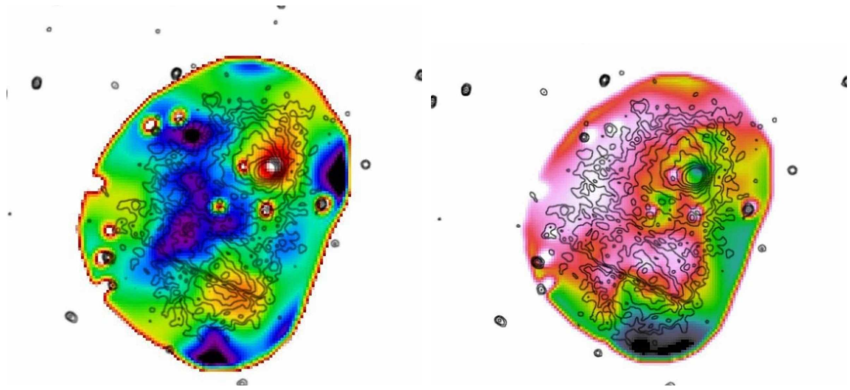

Figure 10: A115: (a) Temperature map (b) metal abundance map.

Abell 3888: This is a Bautz-Morgan type *I-II* and of richness class *0*. It has no cD galaxy (Krick and Bernstein 2006). X-ray images do not show bimodal structures as clear as others (Fig. 7). It is observed for 21.2 ks. Since PN data is not available for this observation, we only use MOS data throughout the analysis. Fig. 8 shows temperature and metal distributions. The hot patchy regions in the south and west are evident.

Abell 115: It has a strong radio source 3C 28.0 in region-A (Gutierrez and Krawczynski 2005). The source is observed with XMM-*Newton* for 44.8 ks. Fig. 9 shows a raw X-ray EPIC image, optical DSS image and radio contours over x-ray. The wavelet temperature and metalicity maps are displayed in Fig. 10. The central region is very hot, decreasing gradually. There are hot region in south and west sides. The ICM has a low metal abundance.

3. DISCUSSION AND CONCLUSION

The X-ray images show two-main bodies clearly. A3705, A2440, A2933 and A115 show similar properties with two clear sub-clusters. There is a high temperature plasma in between these bodies. X-ray peaks are associated with cD elliptical galaxy in most cases, which is the indication of non-disturbance of violent mergers in the central parts. These clusters show the evidences of pre-merger. A115 has also a large scale radio jet. The head of the jet is the hottest region in the ICM. A3888 shows three subclumps of multiple core. There are also small scale temperature variations. These evidences indicate an ongoing activity in the core of A3888.

Acknowledgements

B. Beygu acknowledges the support from TUBITAK, Project No: 106T310 and also the support by Bogazici University Research Foundation via code number 06HB301.

References

Anders, E., Grevesse, N.: 1989, *Geochim. Cosmochim. Acta*, **53**, 197.
Böhringer, H.: 2008, The Universe in X-Rays, eds J. E. Trümper G. Hasinger, Astronomy And Astrophysics Library, Springer – Verlag.
Bourdin, H., Sauvageot J.-L., Slezak, E., et al.: 2004, *Astron. Astrophys.*, **414**, 429.
Gonzalez, A. H. et al.: 2005, *Astrophys. J.*, **618**, 195.
Gutierrez, K., Krawczynski, H.: 2005, *Astrophys. J.*, **619**, 161.
Kolokotronis, V. et al.: 2001, *Mon. Not. R. Astron. Soc.*, **320**, 49.
Krick, J. E., Bernstein, R. A.: 2006, *Astrophys. J.*, **131**, 168.
Mohr, J. J.: 1996, *Astron. J.*, **112**, 1816.
Pratt, G. W., Arnaud, M.: 2003, *Astron. Astrophys.*, **408**, 1.
Snowden, S. L., Kuntz, K. D.: 2007, *Cookbook for Analysis Procedures for XMM-Newton EPIC MOS Observations of Extended Objects and The Diffuse Background*, 2.0.